Title

Experimental study of the U238(S36,3-5n)Hs269-271 reaction leading to the observation of Hs270

Journal

Physical Review C, 81(6)

ISSN

2469-9985

Authors

Graeger, R

Ackermann, D

Chelnokov, M

et al.

Publication Date

2010-06-01

DOI

10.1103/physrevc.81.061601

Peer reviewed

PHYSICAL REVIEW C **81**, 061601(R) (2010)

Experimental study of the ^{238}U(^{36}S,3–5n)$^{269-271}$Hs reaction leading to the observation of ^{270}Hs

R. Graeger,[1] D. Ackermann,[2] M. Chelnokov,[3] V. Chepigin,[3] Ch. E. Düllmann,[2] J. Dvorak,[4] J. Even,[5] A. Gorshkov,[1] F. P. Heßberger,[2] D. Hild,[5] A. Hübner,[2] E. Jäger,[2] J. Khuyagbaatar,[2] B. Kindler,[2] J. V. Kratz,[5] J. Krier,[2] A. Kuznetsov,[3] B. Lommel,[2] K. Nishio,[6] H. Nitsche,[4,7] J. P. Omtvedt,[8] O. Petrushkin,[3] D. Rudolph,[2,5,9] J. Runke,[5] F. Samadani,[8] M. Schädel,[2] B. Schausten,[2] A. Türler,[1,*] A. Yakushev,[1] and Q. Zhi[10]

[1]*Technische Universität München, D-85748 Garching, Germany*
[2]*GSI Helmholtzzentrum für Schwerionenforschung GmbH, D-64291 Darmstadt, Germany*
[3]*Joint Institute for Nuclear Research, RU-141980 Dubna, Russian Federation*
[4]*Lawrence Berkeley National Laboratory, Berkeley, California 94720, USA*
[5]*Johannes Gutenberg Universität Mainz, D-55128 Mainz, Germany*
[6]*Japan Atomic Energy Agency, Tokai-mura, Ibaraki 319–1195, Japan*
[7]*University of California, Berkeley, California 94720, USA*
[8]*University of Oslo, Department of Chemistry, N-0315 Oslo, Norway*
[9]*Lund University, S-22100 Lund, Sweden*
[10]*Institute of Modern Physics, Chinese Academy of Sciences, Lanzhou 730000, People's Republic of China*

(Received 17 March 2010; published 3 June 2010)

The deformed doubly magic nucleus ^{270}Hs has so far only been observed as the four-neutron ($4n$) evaporation residue of the reaction ^{26}Mg + ^{248}Cm, where a maximum cross section of 3 pb was measured. Theoretical studies on the formation of ^{270}Hs in the $4n$ evaporation channel of fusion reactions with different entrance channel asymmetry in the framework of a two-parameter Smoluchowski equation predict that the reactions ^{48}Ca + ^{226}Ra and ^{36}S + ^{238}U result in higher cross sections due to lower reaction Q values, in contrast to simple arguments based on the reaction asymmetry, which predict opposite trends. Calculations using HIVAP predict cross sections for the reaction ^{36}S + ^{238}U that are similar to those of the ^{26}Mg + ^{248}Cm reaction. Here, we report on the first measurement of evaporation residues formed in the complete nuclear fusion reaction ^{36}S + ^{238}U and the observation of ^{270}Hs, which is produced in the $4n$ evaporation channel, with a measured cross section of $0.8^{+2.6}_{-0.7}$ pb at 51-MeV excitation energy. The one-event cross-section limits (68% confidence level) for the $3n$, $4n$, and $5n$ evaporation channels at 39-MeV excitation energy are 2.9 pb, while the cross-section limits of the $3n$ and $5n$ channel at 51 MeV are 1.5 pb. This is significantly lower than the $5n$ cross section of the ^{26}Mg + ^{248}Cm reaction at similar excitation energy.

DOI: 10.1103/PhysRevC.81.061601 PACS number(s): 27.90.+b, 21.10.Tg, 23.60.+e, 25.70.Gh

I. INTRODUCTION

Superheavy elements with proton numbers $Z \geqslant 104$ exist only due to nuclear shell effects, which stabilize them against spontaneous fission (SF). Theoretical calculations predict these shell-stabilization effects to reach a maximum at the closures of the next spherical proton and neutron shells, which are anticipated in the region between $Z = 114$ and $Z = 126$ and at $N = 184$ [1–4]. These effects were long thought to give rise to a so-called island of stability in the midst of a sea of nuclear instability, far away from any nuclei found in nature. More recent calculations based on the macroscopic-microscopic model as well as self-consistent mean-field calculations that also consider deformed nuclear shapes extended this picture and predicted deformed shell closures at $Z = 108$ and at $N = 162$ [5], creating a region of enhanced stability halfway between the heaviest nuclides found on earth and the predicted island of stability. These predictions have been confirmed in recent experiments [6]. The three hassium isotopes $^{269-271}$Hs have been produced in the nuclear fusion reactions ^{248}Cm(^{26}Mg,xn)$^{274-x}$Hs at the GSI [6–9] in Darmstadt. The excitation-function measurement at five different beam energies resulted in maximum cross sections of the $3n$, $4n$, and $5n$ exit channels of about 2.5 pb, 3 pb, and 7 pb, respectively [7].

Recently, the formation of deformed doubly magic ^{270}Hs in the $4n$ evaporation channel in the complete fusion reactions ^{248}Cm(^{26}Mg,$4n$), ^{244}Pu(^{30}Si,$4n$), ^{238}U(^{36}S,$4n$), and ^{226}Ra(^{48}Ca,$4n$) was studied theoretically in more detail using a two-parameter Smoluchowski equation [10]. Simple entrance channel arguments make compound-nucleus (CN) formation appear favorable for systems with larger mass asymmetry, as described in Ref. [11], using quasifission and fusion-fission systematics. However, due to a lower reaction Q value, the reactions ^{238}U(^{36}S,$4n$)^{270}Hs ($\sigma_{\text{theo}} =$ 24 pb) and ^{226}Ra(^{48}Ca,$4n$)^{270}Hs ($\sigma_{\text{theo}} = 30$ pb) are predicted to have higher cross sections compared to the reactions ^{248}Cm(^{26}Mg,$4n$)^{270}Hs ($\sigma_{\text{theo}} = 12$ pb) and ^{244}Pu(^{30}Si,$4n$)^{270}Hs ($\sigma_{\text{theo}} = 8$ pb) [10]. A maximum cross section for the ^{226}Ra(^{48}Ca,$4n$)^{270}Hs reaction of about 30 pb was also predicted in other calculations [12] by using a multidimensional adiabatic potential based on an extended version of the two-center shell model, which has been proven to reproduce experimental

*Current address: Universität Bern and Paul Scherrer Institut, CH-5232 Villigen PSI, Switzerland.

cross sections for various ^{48}Ca-based fusion reactions with actinide targets.

On the contrary, the often-used HIVAP [13] code, which reproduces experimental cross sections within a factor of 2 to 5, predicts a maximum cross section of only 3.5 pb for the reaction $^{36}S + ^{238}U$ for both the 4*n* channel at 38 MeV and the 5*n* channel at about 48-MeV excitation energy, which is comparable to the experimental cross sections for the reaction $^{26}Mg + ^{248}Cm$ [7].

Here, we report first results of an experiment aimed at studying the nuclear fusion reaction $^{36}S + ^{238}U$, which leads to the compound nucleus $^{274}Hs^*$.

II. EXPERIMENT

For the experiment, we used the highly efficient chemical separation and detection system COMPACT which was connected to a recoil chamber (RC) installed behind the ARTESIA target wheel in cave X1 at the GSI [6]. A beam of $^{36}S^{5+}$ ions from an electron-cyclotron resonance source was accelerated by the UNILAC to 256.4 MeV and impinged on a rotating ^{238}U target wheel. A typical beam intensity was 350 particle nA (2.2×10^{12} s^{-1}). The beam passed through a 20.2 μm Be vacuum window and 6 mm of He/O_2 gas mixture ($He:O_2 = 9:1$) at a pressure of 1.1 bar before reaching the target backing. During the experiment, we used two different sets of ^{238}U targets. The first one was deposited on a 12.6 μm Be backing and consisted of three arc-shaped $^{238}U_3O_8$ targets of 1.8 mg/cm^2, 1.5 mg/cm^2, and 1.6 mg/cm^2. These targets were produced by molecular plating. This target wheel had been irradiated with 4.2×10^{18} ^{48}Ca ions prior to our experiment [14]. One of the segments contained 20 μg/cm^2 of ^{nat}Nd for the simultaneous production of α-decaying Os isotopes, a chemical homologue of Hs, for online monitoring of the chemical yield. The second target set was deposited on a 8.2 μm-thick Be backing and consisted of three targets comprising 1.0 mg/cm^2 of metallic ^{238}U each, which had been deposited by sputtering. Due to the oxygen-containing atmosphere, the targets are expected to start oxidizing during the very first moments of beam irradiation. Both targets were measured after the experiment by γ and α measurements as well as by radiography to determine the ^{238}U thickness. Only in one segment from the first target did we observe a loss of approximately 20% of the target material. We assumed that only Hs nuclei exiting the target with a minimum residual range of 10 mm in the gas could be efficiently transported to the detection system. Based on SRIM simulations [15], this corresponds to an active layer of the target of 1.0 mg/cm^2. Thus, the effective target thickness was not affected by the loss of target material. The energy of the ^{36}S ions inside the active target layer was in the range of 175 to 184 MeV within the first set of targets and in the range of 190 to 197 MeV in the second set, corresponding to excitation energies $E^* = (39 \pm 4)$ and (51 ± 3) MeV, respectively [16]. These values are close to the predicted maxima of the 4*n* and 5*n* evaporation channels, respectively [13]. Starting at $E^* = 39$ MeV in the center of the target, we irradiated the first target set with a beam dose of 5.74×10^{17} ^{36}S ions. The second target set was irradiated with a beam dose of 1.03×10^{18} ^{36}S ions at $E^* = 51$ MeV.

The separation of Hs nuclei from other reaction products was achieved with the COMPACT system, which is a highly efficient, rapid chemical-separation and online detection apparatus [6,7] based on the cryo-thermo chromatography method [8,17,18]. Reaction products leaving the target were thermalized in the gas (dried He/O_2, 10% O_2) inside the recoil chamber, which was heated to 350°C. Volatile HsO_4 and OsO_4 were formed and flushed out of the recoil chamber with He/O_2 gas flowing at 1.4 l/min, thereby passing through a 550°C hot quartz wool filter. With this filter, a separation factor of $>10^6$ was attained for the separation from nonvolatile species. Finally, within about two seconds, volatile species were transported to the detection system of COMPACT via an 8-m long per-fluoro-alkoxy Teflon capillary having an inner diameter of 2 mm.

For the detection of the radioactive decay of the separated nuclear reaction products, two similar COMPACT detectors were available. They consisted of two arrays of 32 passivated implanted planar silicon (PIPS) detectors, which were facing each other at a distance of 0.5 mm and embedded in a vacuum-tight two-part Invar enclosure. The active area of each PIPS detector was 9.7 mm × 9.8 mm. Along this channel, a negative temperature gradient from +20°C to −140°C was applied. Based on the known chemical properties of HsO_4 [8], a deposition of transported Hs was expected around −44°C.

For off-line calibration, we used very volatile ^{219}Rn emanating from a ^{227}Ac source. During the experiment, the energy resolution was about 50-keV full width at half maximum. A thin ice layer formed during the experiment on surfaces with temperatures below the dew point, which was typically around −70°C, degrading the energy resolution in the cold part of the detector channel mainly for detector pairs 26 to 32, which were kept at temperatures of −70 to −125°C. Thus, about every 20 hours, the used COMPACT detector was warmed up and dried. During the cleaning of that detector, the other detector was used.

III. RESULTS AND DISCUSSION

The fraction of all produced Os and Hs evaporation residues (EVR) that was detected (i.e., the overall efficiency), which is the product of the chemical yield, transport efficiency, and detection efficiency, was found to be about 50%, similar to that reported in Ref. [6]. For online monitoring of the chemical yield and transport efficiency, we used α-decaying Os isotopes produced via the $^{36}S + ^{nat}Nd$ complete fusion reaction in experiments with the first target set and ^{211}At as well as ^{219,220}Rn produced in transfer reactions and their daughters collected throughout the entire experiment. Due to the chemical separation, only these volatile species and their daughters could be identified in the detectors. We used this background for online monitoring of the experiment as well as for off-line calibration of the α spectra.

We searched for correlated decay chains, which were defined as an α decay ($8.0 \leqslant E_\alpha \leqslant 10.0$ MeV) followed within 300 s in the same or a neighboring detector pair by an α decay in the same energy range or by an SF decay with at least one detected fragment above a threshold of 15 MeV. The energy and time windows were chosen according to the

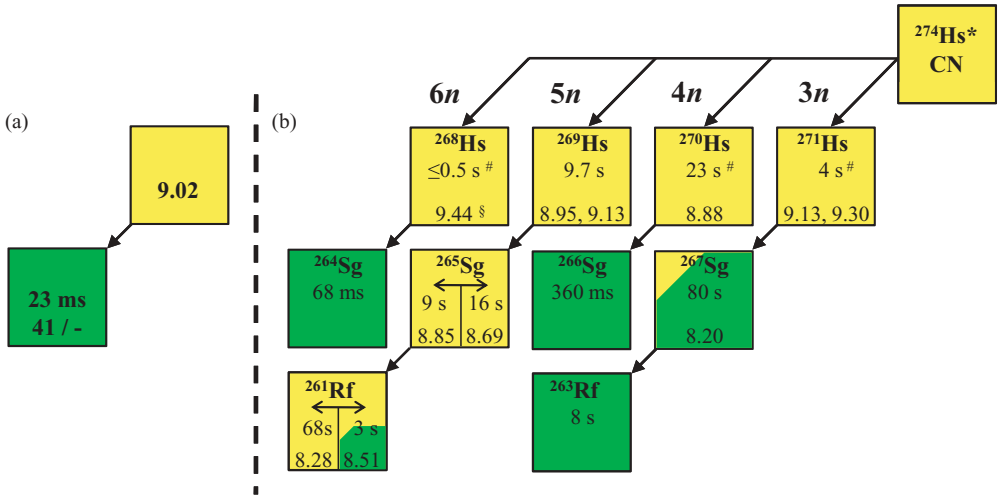

FIG. 1. (Color online) The observed decay chain (a) and known decay properties of the $^{268-271}$Hs isotopes and their daughters (b) [6–8,19]. The half-lives of Hs isotopes marked with a hash (#) were calculated according to the formalism outlined in Ref. [27]. The α-decay energy of ^{268}Hs marked with a paragraph sign (§) is calculated from the Q_α value of ^{268}Hs deduced from Q_α systematics based on all known Hs isotopes [19].

reported decay properties of $^{269,\,270,\,271}$Hs in Refs. [6–8] and ^{268}Hs in Ref. [19] shown in Fig. 1(b).

Because of the background, pseudocorrelated chains can be found with nonzero probability. Based on our measured event rates in the energy regions of interest, we calculated the probability to observe random decay chains of the type α-α-α-α, α-α-SF, and α-SF satisfying the energy and time criteria specified above. The results are summarized in Table I. In the energy interval just mentioned, 351 and 771 α particles were registered in the first and the second run, respectively. They originated mainly from α decays of ^{212}Po, a daughter of ^{220}Rn. Also, 6 SF-fragment-like (SFf) events were registered in the first run and 13 SFf-like events were registered in the second run. None of these were coincident with each other. The detection efficiency for at least one fragment is 95%; for both fragments, it is 76%.

Hence, the probability to always register only one fragment out of 6 or 13 SFf events was determined to be extremely low (5×10^{-5} and 5×10^{-10}, respectively). Thus, the SFf-like background originated mostly from background radiation induced by cosmic radiation or possibly electronic noise and not from real fission events.

The data analysis revealed only one correlated decay chain at the higher excitation energy $E^* = 51$ MeV. A $9.02^{+0.05}_{-0.10}$-MeV α particle was observed in the bottom detector #24 and was followed after 23 ms by one 41-MeV fission fragment measured in the top detector #24, as illustrated in Fig. 1(a). The temperature of that detector was around -60°C, which is situated in the temperature range where hassium atoms have been deposited in former experiments [6–8]. Furthermore, no contaminations from nonvolatile actinides and minor transactinides were observed. Also, the α-decay energy of about 9 MeV points to a hassium decay.

TABLE I. Number of expected randomly correlated background events forming chains of the type given in the first column. The correlation time between two members of one decay chain in the correlation search using subsequent time windows is Δt.

Decay Chain	$E^* = 39$ MeV	$E^* = 51$ MeV	Δt (s)
$\alpha \cdot \alpha \cdot \alpha \cdot \alpha$	7.1×10^{-4}	3.1×10^{-3}	300
$\alpha \cdot \alpha$·SF	4.6×10^{-3}	1.7×10^{-3}	300
α·SF	1.6×10^{-2}	4.6×10^{-2}	300
α·SF (^{270}Hs)	1.1×10^{-4}	3.1×10^{-4}	2

The energy and energy resolution of detector pair #24, bottom, where the relevant α particle was observed, was calibrated off-line with ^{219}Rn-^{215}Po decay chains, measured in the same detector pair, occurring in a time window around this event. At $E^* = 51 \pm 3$ MeV, ^{270}Hs, ^{269}Hs, and ^{268}Hs formed in the 4n, 5n, and 6n exit channels, respectively, are expected, according to HIVAP, to be produced with significant cross sections of about 0.2 pb, 3.5 pb, and 0.2 pb, respectively. The observation of other exit channels at this excitation energy is highly unlikely because expected cross sections are at least about a factor of 10 lower.

Below, the possible assignment to one of the aforementioned channels is discussed. The SF following 23 ms after the α emission may be attributed to the decay of ^{264}Sg, as it is quite compatible with the reported half-life of ^{264}Sg of $T_{1/2} = 68^{+37}_{-18}$ ms [20,21]. This assignment implies a preceding α decay of ^{268}Hs, produced in the 6n evaporation channel. From interpolations of Q_α value systematics of all known Hs isotopes, an α-decay energy of about 9.58 MeV can be deduced [19]. Because of the significant deviation between this value and the measured α-particle energy of $9.02^{+0.05}_{-0.10}$ MeV, ^{268}Hs can quite certainly be excluded as the correct assignment. From results of a chemical search experiment for this nuclide, it follows that its half-life is most likely $\leqslant 0.5$ s [19], which is short compared to the transport time of the experimental setup ($\sim$2 s). This significantly reduces the overall efficiency for such short-lived species. Hence, assignment to ^{268}Hs would imply the cross section for the 6n evaporation channel to be much higher than that for the 5n evaporation channel, in

contrast to expectations based on hot fusion excitation function systematics.

The measured α decay could thus be attributed to the decay of ^{269}Hs or ^{270}Hs. The well-known decay of ^{269}Hs, produced in the 5n exit channel, consists of two successive α decays from ^{269}Hs and ^{265}Sg followed by either an α decay or SF of ^{261}Rf [6,22]. Assuming that we only detected the first α decay of ^{269}Hs and SF of ^{261b}Rf, while missing the α decay of ^{265}Sg, the measured α-particle energy is consistent with a reported α-particle energy of ^{269}Hs of 8.95 MeV [7]. However, the observed correlation time is much shorter than expected for such an incomplete ^{269}Hs decay chain based on the known half-lives of ^{265}Sg and ^{261b}Rf. In addition, due to the high detection probability of a single α particle, the probability to miss an α particle within a decay chain is low.

The last possibility is the decay of ^{270}Hs, produced via the 4n exit channel. The measured α-decay energy again fits quite well with the reported value of 8.88 ± 0.05 MeV from chemistry experiments [7]. In addition, the observed correlation time is compatible with the reported half-life of ^{266}Sg of about 360 ms [7]. In conclusion, we tentatively associate the presently observed decay chain with decays of a ^{270}Hs nucleus and its daughter ^{266}Sg.

According to this assignment, the measured lifetime of ^{266}Sg is several orders of magnitude lower than the time window of 300 seconds, which was chosen for the event search for all possible decay chains from $^{268-271}$Hs. A more realistic calculation of the number of expected randomly correlated chains using a time window of five ^{266}Sg half-lives (2 s) can also be found in Table I. Therefore, the probability that the observed α-SF decay chain is of random origin is negligible.

At $E^* = 39$ MeV, no event was observed; the upper cross-section limit for the 3n, 4n, and 5n evaporation channels at this energy is 2.9 pb. The cross section for the 4n channel at $E^* = 51$ MeV based on the one observed event is $0.8^{+2.6}_{-0.7}$ pb and the cross-section limit for the 3n and 5n channel is 1.5 pb. Errors and limits of measured cross sections correspond to the 68% confidence level [23].

The measured cross section at $E^* = 51$ MeV and the limit at $E^* = 39$ MeV for the ^{238}U(^{36}S,4n)^{270}Hs reaction are comparable to measured cross sections of the reaction ^{248}Cm(^{26}Mg,4n)^{270}Hs [7]. The cross-section limits for the ^{238}U(^{36}S,5n)^{269}Hs reaction at 51-MeV and 39-MeV excitation energy are comparable to or even lower than the cross section of the ^{248}Cm(^{26}Mg,5n)^{269}Hs reaction [7]. However, our results are in contrast to the predictions of Ref. [10]. The measured cross section and cross-section limits are more than one order of magnitude lower than the predicted peak cross section of 24 pb derived in Ref. [10].

For the ^{248}Cm(^{26}Mg,4n)^{270}Hs reaction, Ref. [10] predicted a peak cross section of about 12 pb, half that of the ^{238}U(^{36}S, 4n)^{270}Hs reaction. According to [10], the higher peak cross section for the latter reaction compared with the former one should be driven by Q-value effects. Our measurement excludes such a trend and furthermore contradicts quantitatively and qualitatively the predictions and conclusions made by Ref. [10]. They agree better with HIVAP calculations—within a factor of 2 to 3.

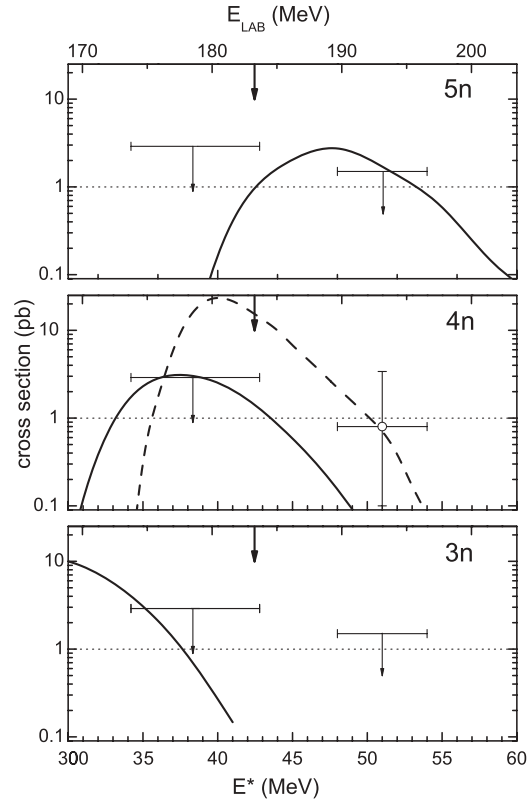

FIG. 2. Production cross sections and limits measured for the reaction ^{238}U(^{36}S, xn)$^{274-x}$Hs in comparison with HIVAP calculations (solid line) and predictions from Ref. [10] (dashed line). Arrows indicate the location of the Bass fusion barrier.

A summary of experimental results compared with theoretical predictions is provided in Fig. 2.

According to Ref. [12], the cross section for evaporation-residue production in nuclear fusion reactions can be described as the sum over all partial waves of the product of the penetrability of the multidimensional Coulomb barrier, the probability of compound nucleus formation, and the survival probability during the deexcitation of the compound nucleus via successive neutron evaporation. Whereas the first two terms of the product reflect the formation process (entrance channel), the third term depends on the properties of the CN and members of the evaporation cascade. Because both fusion reactions ^{36}S + ^{238}U and ^{26}Mg + ^{248}Cm result in the same CN (^{274}Hs), the exit channel is nearly identical for both reactions at the same excitation energy (neglecting small differences in angular momentum of the compound nucleus after its formation) and could not explain possible differences in the cross sections. Hence, they must be due to the entrance channel. We observed one ^{270}Hs event at $E^* = 51$ MeV, above the Coulomb barrier, where the difference in the CN-formation probability, which depends mainly on the asymmetry of the projectile-target combination, is expected to be the dominant factor.

Large sub-barrier fusion enhancement was observed in the reaction ^{26}Mg + ^{248}Cm [7] and also in recent experiments concerning orientation and coupled-channels effects on the

production of superheavy elements in fusion reactions with ^{238}U targets [20,24,25]. The measurement of a complete excitation function including measurements at lower excitation energies below the Bass barrier would help for a deeper understanding of ^{238}U-based fusion-evaporation residue reactions, as well as sub-barrier fusion systematics with ^{238}U targets. Especially, the influence of the deformation of the projectile on sub-barrier fusion would be very interesting to explore. It seems that in this reaction, the maximum cross section of the 4*n* evaporation channel is probably higher than the maximum 5*n* evaporation channel, in contrast to former investigations of ^{238}U-based hot fusion EVR reactions [21,26].

ACKNOWLEDGMENTS

We would like to thank the UNILAC crew for providing stable and intense ^{36}S beams. This work was supported by the German Bundesministerium für Bildung und Forschung (BMBF Projects No. 06MP247I and 06MZ223I). Financial support for J. Dvorak was provided by the Office of High Energy and Nuclear Physics, Nuclear Physics Division, of the US Department of Energy, under contract DE-AC03-76SF00098. F. Samadani and J. P. Omtvedt gratefully acknowledge financial support from the Norwegian Research Council under project number 148994/V30.

[1] S. Cwiok *et al.*, Nucl. Phys. A **611**, 211 (1996).
[2] W. D. Myers *et al.*, Nucl. Phys. A **601**, 141 (1996).
[3] A. Sobiczewski, Acta Phys. Pol. B **29**, 2191 (1998).
[4] K. Rutz *et al.*, Phys. Rev. C **56**, 238 (1997).
[5] Z. Patyk and A. Sobiczewski, Nucl. Phys. A **533**, 132 (1991).
[6] J. Dvorak *et al.*, Phys. Rev. Lett. **97**, 242501 (2006).
[7] J. Dvorak *et al.*, Phys. Rev. Lett. **100**, 132503 (2008).
[8] Ch. E. Düllmann *et al.*, Nature (London) **418**, 859 (2002).
[9] A. Türler *et al.*, Eur. Phys. J. A **17**, 505 (2003).
[10] Z. H. Liu and J.-D. Bao, Phys. Rev. C **74**, 057602 (2006).
[11] M. G. Itkis *et al.*, Nucl. Phys. A **787**, 150c (2007).
[12] V. Zagrebaev and W. Greiner, Phys. Rev. C **78**, 034610 (2008).
[13] W. Reisdorf and M. Schädel, Z. Phys. A **343**, 47 (1992).
[14] R. Eichler *et al.*, Radiochimica Acta **94**, 181 (2006).
[15] J. F. Ziegler, Nucl. Instrum. Methods A **219**, 1027 (2004).
[16] G. Audi *et al.*, Nucl. Phys. A **729**, 337 (2003).
[17] U. W. Kirbach, Nucl. Instrum. Methods A **484**, 587 (2002).
[18] Ch. E. Düllmann *et al.*, Nucl. Instrum. Methods A **479**, 631 (2002).
[19] J. Dvorak *et al.*, Phys. Rev. C **79**, 037602 (2009).
[20] K. Nishio *et al.*, Eur. Phys. J. A **29**, 281 (2006).
[21] K. E. Gregorich *et al.*, Phys. Rev. C **74**, 044611 (2006).
[22] Ch. E. Düllmann and A. Türler, Phys. Rev. C **78**, 029901 (2008).
[23] K.-H. Schmidt *et al.*, Z. Phys. A **316**, 19 (1984).
[24] K. Nishio *et al.*, Phys. Rev. Lett. **93**, 162701 (2004).
[25] K. Nishio *et al.*, Phys. Rev. C **77**, 064607 (2008).
[26] J. M. Gates *et al.*, Phys. Rev. C **77**, 034603 (2008).
[27] A. Parkhomenko and A. Sobiczewski, Acta Phys. Pol. B **36**, 3095 (2005).